CHEMISTRY
A European Journal

A Journal of
ChemPubSoc Europe

Accepted Article

Title: FeIII–salen based Probes for the Selective and Sensitive Detection of E450 in Foodstuff

Authors: Felix Hubertus Zelder, Gilles Gasser, Prerna Yadav, Marta Jakubaszek, Bernhard Spingler, and Bruno Goud

To be cited as: *Chem. Eur. J.* 10.1002/chem.201905686

Link to VoR: http://dx.doi.org/10.1002/chem.201905686

Supported by
ACES

WILEY-VCH

10.1002/chem.201905686

Fe^{III}–salen based Probes for the Selective and Sensitive Detection of E450 in Foodstuff

Prerna Yadav,[a] Marta Jakubaszek,[b,c] Prof. Dr. Bernhard Spingler,[a] Dr. Bruno Goud,[c] Dr. Gilles Gasser,[b] and Prof. Dr. Felix Zelder[a*]

[a]*Department of Chemistry, University of Zurich, Winterthurerstrasse 190, CH-8057 Zurich, Switzerland. Fax: +41 44 635 6803; E-mail: felix.zelder@chem.uzh.ch, www.felix-zelder.com.*

[b]*Chimie ParisTech, PSL University, CNRS, Institute of Chemistry for Life and Health Sciences, Laboratory for Inorganic Chemical Biology, 11, Rue Pierre et Marie Curie, F-75005 Paris, France*.

[c]*Institut Curie, PSL University, CNRS UMR 144, Paris, France*.

Abstract

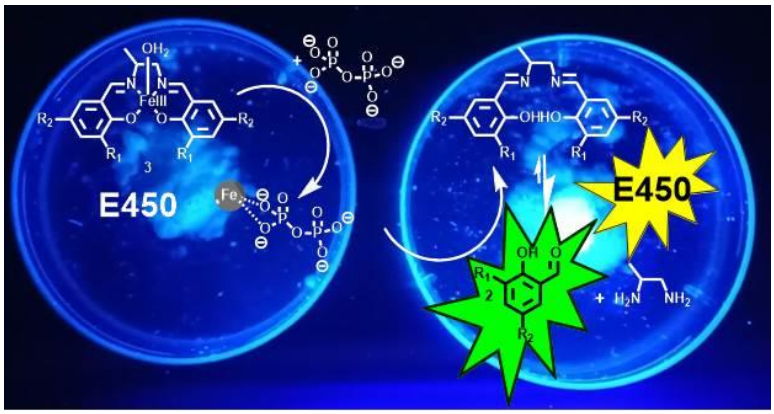

Inorganic pyrophosphate (PPi) is considered as a diagnostic marker for various diseases such as cancer and vascular calcification. It plays also an important preservative role as an additive E450 in foodstuff. In this work, we describe a novel selective Fe^{III}-salen based probe for PPi, which disassembles in the presence of the target analyte into its molecular blocks, 1,2-propanediamine and 3-chloro-5-formyl-4-hydroxybenzenesulfonic acid. The latter signaling unit leads to a fluorometric response. Compared to a related prototype, the new complex shows a 2.3-times stronger emission at 500 nm and a 155-times better selectivity of PPi over ATP. Importantly, the new probe was successfully applied for detecting E450 in foodstuff.

Keywords: Pyrophosphate (PPi), Fe^{III}-salen complex, Sensing, Disassembly approach, Reaction based probe, E450.

10.1002/chem.201905686

Introduction

Phosphates are ubiquitous in biological systems. They are encountered as mono- and poly-anions as well as building blocks in natural products such as nucleic acids, adenosine triphosphate (ATP) and vitamin B_{12}.[1, 2] Related to their diverse molecular structures, this class of compounds exhibits important biological roles in energy storage and signal transduction processes.[3, 4] One member of this important class of compound is inorganic pyrophosphate (PPi; $P_2O_7^{4-}$).[5] It is produced from nucleoside triphosphates in various biological transformations including the hydrolysis of ATP, the syntheses of DNA as well as of small molecular metabolites.[5, 6] Considering the broad occurrence of (polyoxo)phosphates in biological systems, they are also encountered as natural composites in food. In addition to their natural occurrence, this class of compounds is also legally added to foodstuff as preservative, emulsifier or taste intensifier.[7] In the European Union and Switzerland, the use of PPi as food additive E450 is not restricted and PPi is found in high concentrations in products such as canned meat, fish and bakery products.[8] Although the dietary intake of naturally occurring (polyoxo)phosphates does not represent a risk for healthy people,[9] the increasing use of phosphate salts as food additives exposes risks to people with renal disorders and cardiovascular diseases.[8, 10, 11] For this reason, the restriction of dietary phosphate is recommended for patients with chronic renal failures for many years.[8, 10, 11]

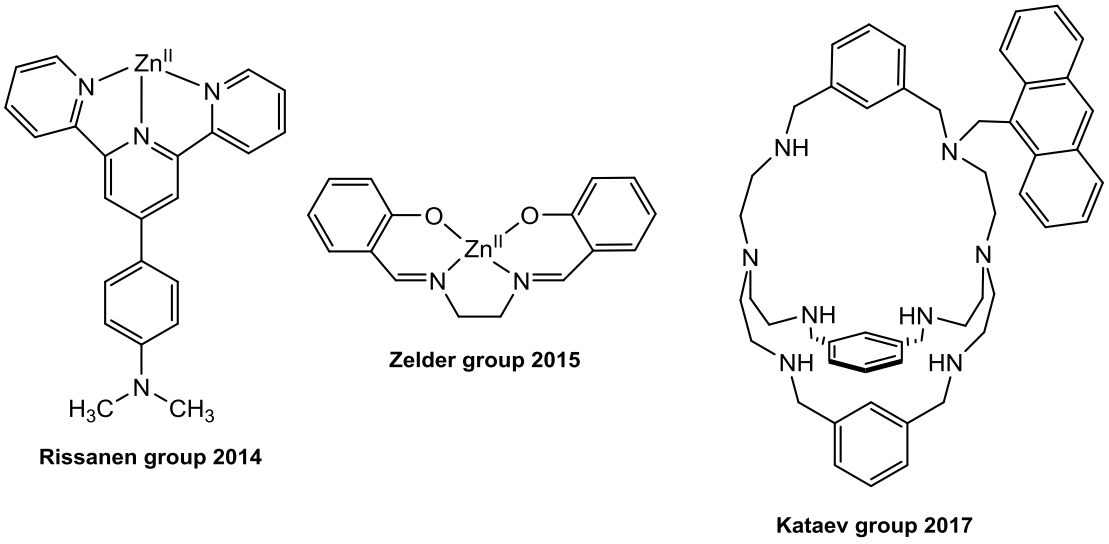

Figure 1: Examples of fluorogenic probes for PPi detection.[12-14]

All of these examples underscore the importance to monitor (polyoxo)phosphates in the environment, biological systems and foodstuff. In this line, the development of straightforward selective and sensitive probes for PPi has attracted considerable attention.[1, 15-17] The most

10.1002/chem.201905686

common sensing strategies are probably the chemosensing and displacement approaches for colorimetric as well fluorometric PPi detection.[18] In 1994, Czarnik reported on the fluorometric detection of PPi with a polyamine modified anthracene derivative in H_2O.[19] The Kataev group described the encapsulation and detection of PPi with an azacryptand based receptor (Figure 1, right).[14] Probably the first example of discrimination of PPi over ATP was reported in 2004 by Hong and coworkers using a binuclear Zn^{II}-bis(2-pyridylmethyl)amine complex. This system showed an approximate 5-fold fluorescence enhancement upon binding of PPi compared to ATP.[20-22] Recently, a similar relative increase in emission intensity was observed for an aspartic acid-functionalized perylene diimide Cu^{II}-aggregate in the presence of PPi over ATP (~ 4-fold).[23] Despite the large number of PPi sensors described so far in the literature,[24-26] only few detect endogenous PPi in biological media. Rissanen`s terpyridine-Zn^{II} complex (Figure 1, left) is one of the rare exceptions.[12] Our group contributed to this area with Zn^{II}-, and Fe^{III}-salen complexes as disassembly probes for PPi (Figure 1, middle).[13, 27-30] Herein, we report on a new Fe^{III}-salen complex **3** as reaction based sensor[31-34] with improved sensitivity and selectivity for PPi (Scheme 1) and demonstrate its applicability for detecting PPi as E450 in baking powder. Remarkably, a single methyl group at the ethylene diamine backbone of the probe led to a 155 times enhanced selectivity of PPi over ATP.

Concept:

The structures of the Fe^{III}-salen based probes **1**-**4** are shown in Scheme 1. We envisaged that probes **2**-**4** would disassemble in the presence of PPi to their molecular building blocks according to the mechanism depicted in Scheme 1. Initially, PPi extracts the central Fe^{III}-ion from the probes ("unlocking"). The metal-free tetradentate ligands **6**-**8** then hydrolyse to the diamine subunit and the fluorescent salicylaldehyde derivative **10** ("disassembly"). In short, "unlocking" of the Fe^{III}-salen based probes ("locked complexes") transduces PPi into a detectable, fluorescent signal.

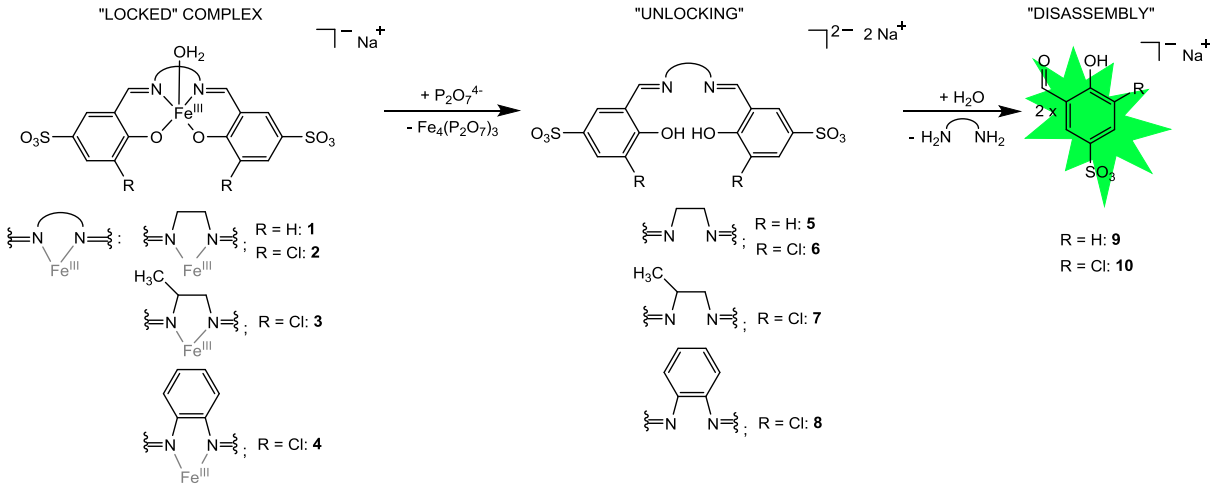

Scheme 1: Structures of the Fe^{III}-probes **1-4** and its disassembly to the fluorescent salicylaldehyde derivatives **9**, **10** in the presence of PPi.

This mode of PPi detection was previously demonstrated with prototype **1** releasing the signaling unit **9**.[27] Unfortunately, this reaction-based probe exhibits several drawbacks. In particular, the sensitivity of **1** for PPi was rather poor. This undesired behavior is attributed to the weak fluorescence of **9** (Φ = 0.13 in DMF).[35] To overcome this limitation, we decided to synthesize probes **2-4** with a more fluorescent signaling subunit **10** instead of **9**. This derivative contains a chloro instead of a hydrogen substituent at position C3 of the salicylaldehyde moiety. This subtle, but important change leads to a 2.7-fold increase in quantum yield of the signaling unit **10** (Φ = 0.35 in DMF) compared to **9**.[35] In addition, we speculated also to implement additional modifications into the ethylenediamine backbone of **2** for fine-tuning the selectivity and reactivity of the probes. For this purpose, we chose to decorate **3** with an additional, electron donating methyl group in the ethylenediamine subunit and decided to replace the latter with a phenylenediamine building block in compound **4**.

Synthesis of Fe^{III}-probes: Prototype **1** with the signaling unit **9** was synthesized as described previously.[36] The signaling unit 3-chloro-5-formyl-4-hydroxybenzenesulfonic acid **10** was prepared as its sodium salt in three steps in 48 % yield according to literature procedures.[37] Afterward, this building block was condensed in EtOH/H_2O (4:1) with either ethylenediamine, 1,2-propanediamine or phenylenediamine to give ligands **6-8** in good yields (yields: 75-83%). The corresponding Fe^{III}-complexes **2-4** were then obtained by complexation of the ligands with $FeCl_3$ (yields: 83-88%). The synthetic route for the preparation of **3** is schematically depicted in Scheme 2.

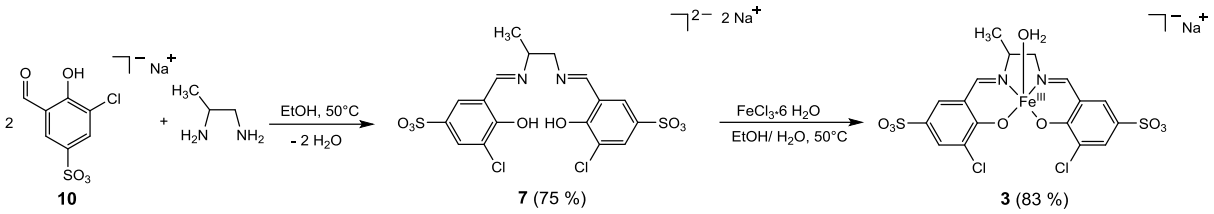

Scheme 2. Synthesis of the Fe^{III}-probe **3** from the signaling unit **10** and 1,2-propanediamine.

In the high-resolution mass spectrum of **3**, the $[M–Na-H_2O]^{2-}$ ion was observed at *m/z* 280.93908, corresponding to the molecular formula $C_{17}H_{12}Cl_2FeN_2O_8S_2^{2-}$ (m/z_{calc} 280.93862). This behavior suggests that Fe^{III} is reduced to Fe^{II} during mass spectrometric analysis. The absorption spectrum of **3** in H_2O (pH 5, [Robinson buffer] = 10 mM) exhibits maxima at 310, 395 and 500 nm. The latter maximum was assigned to a ligand-to-metal-charge transfer (LMCT) band and showed reversible changes with variations in pH (Figure S1). The pK_a of the Fe^{III}-bound water of **3** was determined as 6.9 (Figure S2).

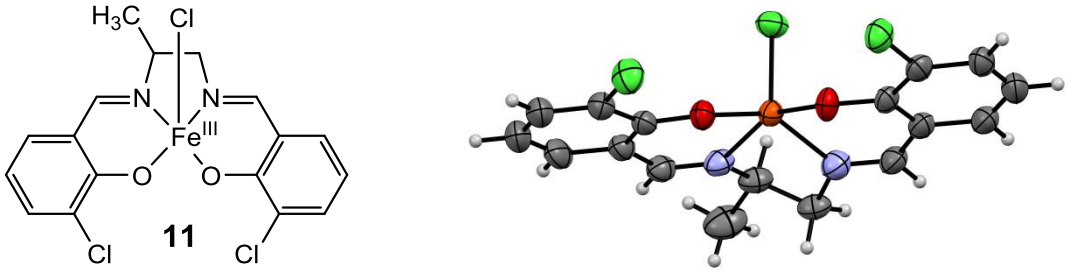

Figure 2: Structure of the Fe^{III}-probe **11** (*left*) and its X-ray crystal structure (*right*). Ellipsoidal plot with a probability of 50%. One out of two molecules in the asymmetric unit is shown. Disorder in the propylene linker moiety is omitted for clarity.

This behavior is in agreement with related square-pyramidal Fe^{III}-complexes containing an apical aqua ligand.[38-47] Further structural information was obtained from crystal structure analysis. Since all our attempts failed to crystallize complex **3**, we decided to prepare the related hydrophobic ferric chloride - complex **11** (Figure 2 *left*). This derivative contains a chlorido instead of an aqua ligand at the metal center and lacks the sulfonate functionalities in the salicyaldehyde subunit compared to **3**. Compound **11** was successfully crystallized from MeOH/ hexane using the layering method[48] and structural analysis supported the square pyramidal coordination geometry of the complex (Figure 2 *right*, Figure S3, Tables S1, S2). Complexes **2**-**4** were also analyzed by HRMS, IR and UV-Vis spectroscopy (Figures S4-S9).

.

Transformations of the Probes in the Presence of PPi:

We tested the disassembly of the probes **2-4** (16 μM) with PPi (10 equiv) using UV-Vis and fluorescence spectroscopy. Addition of the target analyte PPi to the probes led to the formation of a new absorption band at 385 nm (Figure S10 *left*) and to a 2.4 and 3.5-fold enhanced fluorescence emissions at 500 nm for **2** and **3** (Figure S10 *right*), respectively.

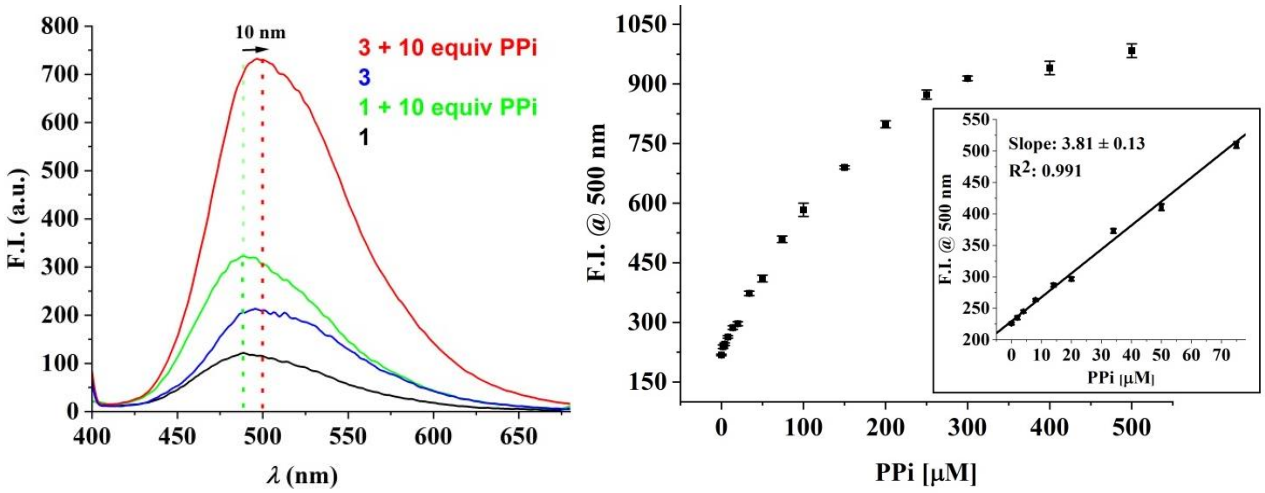

Figure 3. *Left:* Fluorescence spectra of **1** (16 μM) and **3** (16 μM) before and after addition of PPi (10 equiv; incubation time: 30 min; λ_{ex} (**1**) = 350 nm, λ_{ex} (**3**) = 385 nm) at pH 7.4 ([Tris buffer] = 10 mM). *Right:* Change in fluorescence intensity of **3** in the presence of PPi (0-500 μM) at 500 nm. *Inset:* Corresponding calibration curve (**3** (16 μM), PPi (0-75 μM); LOD = 1.50 μM, R^2 = 0.991).

These spectral changes are attributed to the PPi-induced liberation of the signaling unit **10** from **2** and **3** (Figure S11). This behavior was also confirmed for the disassembly of **3** by mass spectrometric methods indicating the formation of **10** ($[M–Na]^-$: *m/z* 234.94741, m/z_{calc} 234.94730) (Figure S12). In comparison to the disassembly of prototype **1** with PPi (10 equiv), the reaction with **3** leads to a 2.3-times stronger emission and a red shift (10 nm) of the emission maximum (Figure 3 *left*). This significant improvement is in line with the release of the 2.7-times more fluorescent signaling unit **10** instead of **9** from the "locked" Fe^{III}-salen complexes. A calibration curve was generated from titrations of **3** (16 μM) with increasing concentrations of PPi (0-500 μM) indicating that quantifications are possible in the linear range between 0 and

75 µM of PPi with a limit of detection (LOD) of 1.50 µM (Figure 3 *right*). In contrast to the reactivity of probes **3** and **2**, complex **4** did not show any tendency to disassemble in the presence of PPi (Figure S13). Apparently, the strong electron donating character of the phenylenediamine backbone enhances coordination of the Fe^{III}-ion and impedes thereby the extraction of the metal ion.

Selectivity Studies:

The selectivity of the Fe^{III}-complexes **2** and **3** for PPi was tested subsequently with sixteen frequently encountered anions including the phosphate ions ATP and PO_4^{3-} (Figures 4, S14 and S15). Complex **2** showed unfortunately a 1.4-fold and 1.2-fold increase in fluorescence at 500 nm in the presence of ATP and PO_4^{3-} (Figure S14 *right*).

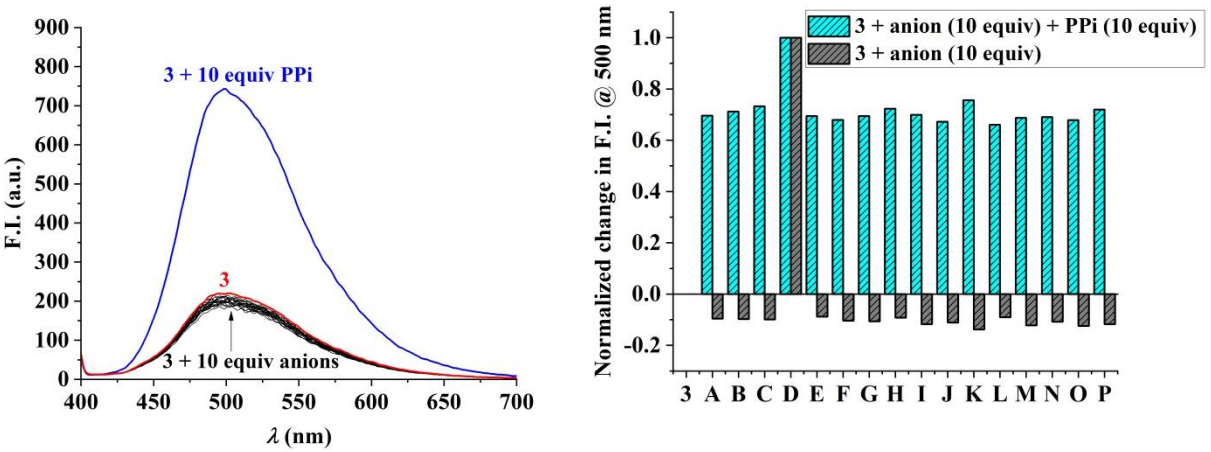

Figure 4. *Left:* Fluorescence spectra of **3** (16 µM, λ_{ex} = 385 nm) in the presence of PPi (10 equiv) and 16 different anions (10 equiv; see *right* for details; incubated for 30 min) at pH 7.4 ([Tris buffer] = 10 mM). *Right:* Normalized change in fluorescence intensity of **3** (16 µM, λ_{ex} = 385 nm) at 500 nm in the presence of PPi (10 equiv) and different anions (10 equiv) at pH 7.4 ([Tris buffer] = 10 mM) (**A**: AMP, **B**: ADP, **C**: ATP, **D**: PPi, **E**: PO_4^{3-}, **F**: CN^-, **G**: F^-, **H**: Cl^-, **I**: I^-, **J**: Br^-, **K**: SO_4^{2-}, **L**: NO_3^-, **M**: CO_3^{2-}, **N**: CH_3COO^-, **O**: SCN^- and **P**: HCO_3^-).

This lack of selectivity was significantly improved with probe **3.** This fluorescent probe for PPi showed – *in contrast to* **2** - no disassembly with all other anions including ATP and PO_4^{3-}

(Figure S15, Figure 4). The selectivity of **3** for PPi in the presence of other potentially competing anions was additionally underscored in competition assays (Figure 4).

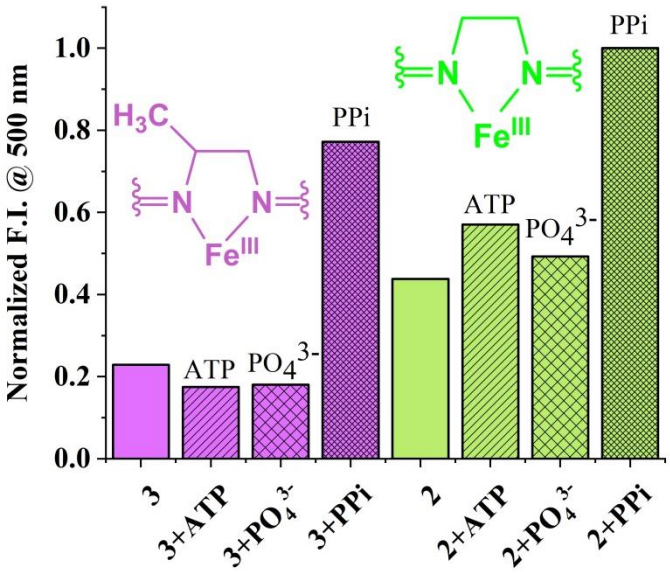

Figure 5. Fluorescence intensity at 500 nm of **3** and **2** (16 μM; λ_{ex} = 385 nm) in the absence and presence of PPi, ATP and PO_4^{3-} (10 equiv; incubated for 30 min) at pH 7.4 ([Tris buffer] = 10 mM).

In comparison to complex **2**, compound **3** with an additional methyl group in the ethylenediamine backbone of the salen ligand exhibited a remarkable improved selectivity of PPi over ATP (~ 130 fold) and PO_4^{3-} (~ 55 fold) as depicted in Figure 5.

Mechanistic Studies:

The disassembly reaction of **3** to the signaling unit **10** in the presence of PPi (Scheme 1) was supported by ^{1}H-NMR studies in D_2O and mixtures of DMSO-d_6 and D_2O. Addition of PPi (10 equiv) to a solution of **3** (2 mM) at *p*D 7.4 ([Tris buffer] = 10 mM) showed in the ^{1}H-NMR spectra the formation of **10** within 30 min (Figure S16). Remarkably, we did not observe any signals from the metal-free ligand **7** in the reaction mixtures. This behavior suggests that upon extraction of Fe^{III} from **3** with PPi, the subsequent hydrolysis of **7** with H_2O is fast on the NMR time scale. In contrast, we were able to observe the formation of **7** when we demetalled **3** with PPi in DMSO-d_6 (Figure 6). This time, two singlets at 8.60 ppm and 8.65 ppm (Figure 6) were

observed corresponding to the protons (labeled as *a* and *a'*, respectively) of the imine moiety of **7**. Hydrolysis of the latter to the signaling unit **10** was only observed after adding increasing amounts of D_2O (5-15 µL) to the reaction mixture (Figure 6: lines 3-5). Evidence for interactions of Fe^{III} with the bidentate chelator PPi was also obtained by ^{31}P NMR indicating a high field shift of 0.73 ppm along with a broadening of the singlet at -7.71 ppm (Figure S17).

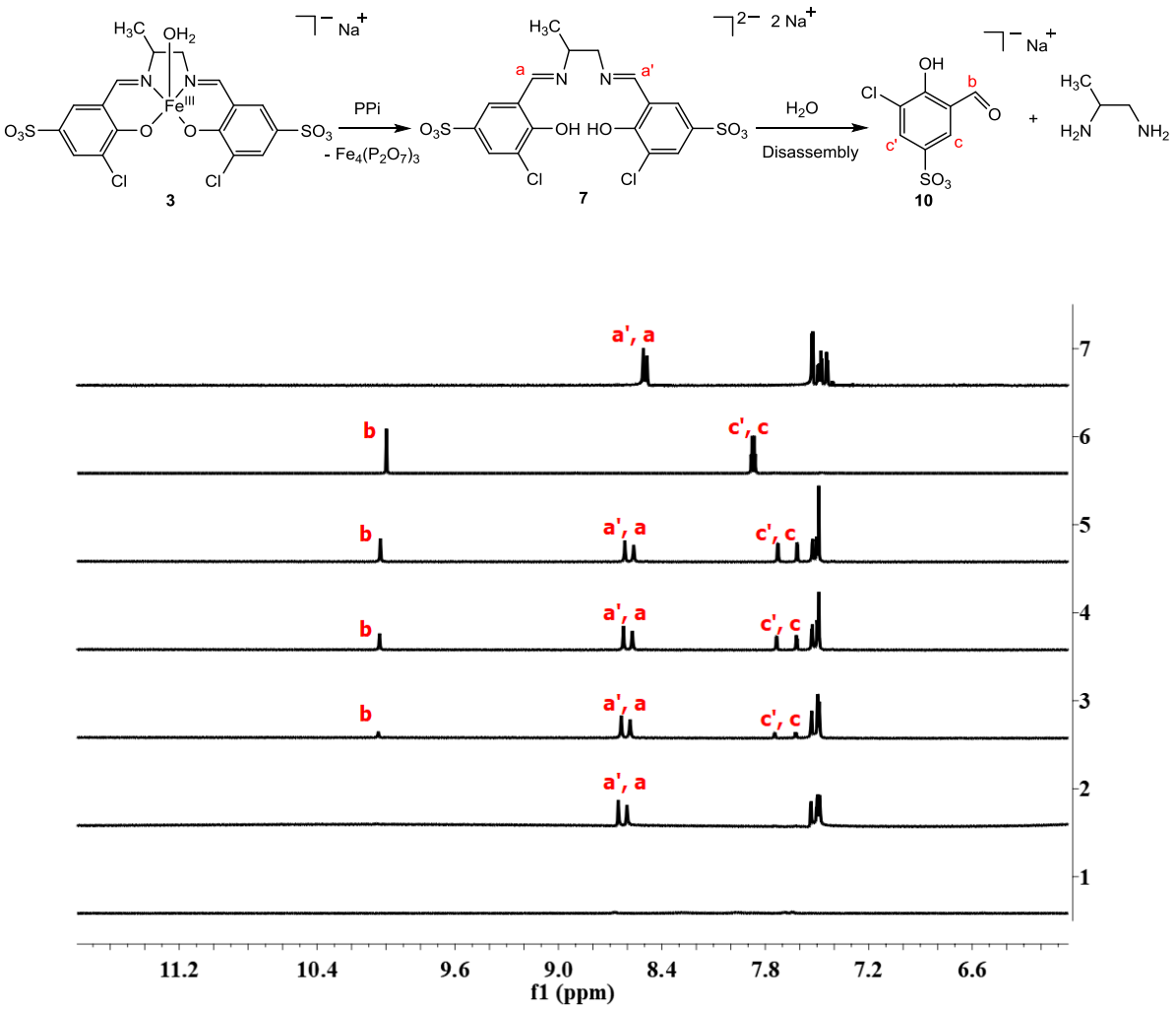

Figure 6. *Top:* Scheme for the reaction of **3** with PPi to form the salicylaldehyde derivative **10**. *Bottom:* ^1H NMR spectra of **3** (2 mM, in DMSO-d_6) in the absence [line 1] and presence of PPi (10 equiv) in DMSO-d_6 [line 2]. Lines 3 to 5: Addition of increasing amounts of D_2O (5, 10 and 15 µL) to the reaction mixture depicted in line 2. Line 6 corresponds to a solution of **10** in D_2O and line 7 corresponds to a solution of **7** in DMSO-d_6 for comparison.

10.1002/chem.201905686

Kinetics of the disassembly of **3** with PPi was determined by UV/Vis spectroscopy. When PPi (20 equiv) was added to a solution of **3** (16 μM) in H_2O at pH 7.4 ([Tris] = 10 mM) at 25 °C, clean conversion to **10** within 50 min was observed by monitoring spectroscopically changes at 385 nm. A monoexponential fit (R^2= 0.992) yielded a pseudo-first-order rate constant (k_{obs}) of 0.0567 ± 8.7084×10^{-4} min^{-1} with a half-life time ($t_{1/2}$) of 12 min (Figure 7). This rate is about 44 times faster than self-hydrolysis of **3** in the absence of any analyte at pH 7.4 at 25 °C (k_{obs} = 0.0013 ± 1.3038×10^{-5} min^{-1}, $t_{1/2}$ = 533 min) (Figure S18). The stability of the complex **3** was studied from pH 5.5 to 10.5 demonstrating that the complex is less susceptible to self-hydrolysis at lower pH (Table S3). In contrast, disassembly of **3** in the presence of ATP (20 equiv) at pH 7.4 at 25 °C is only 2.8 times faster than background hydrolysis (k_{obs} = 0.0036 ± 2.4201×10^{-5} min^{-1}, $t_{1/2}$ = 193 min) (Figure S19). We assign this behavior to mainly two factors. On the one hand, to a higher charge density of PPi over ATP and on the other hand to a subtle, but important entropic stabilization of **3** against demetallation. We are currently performing additional detailed mechanistic studies to explicitly unravel this important effect.

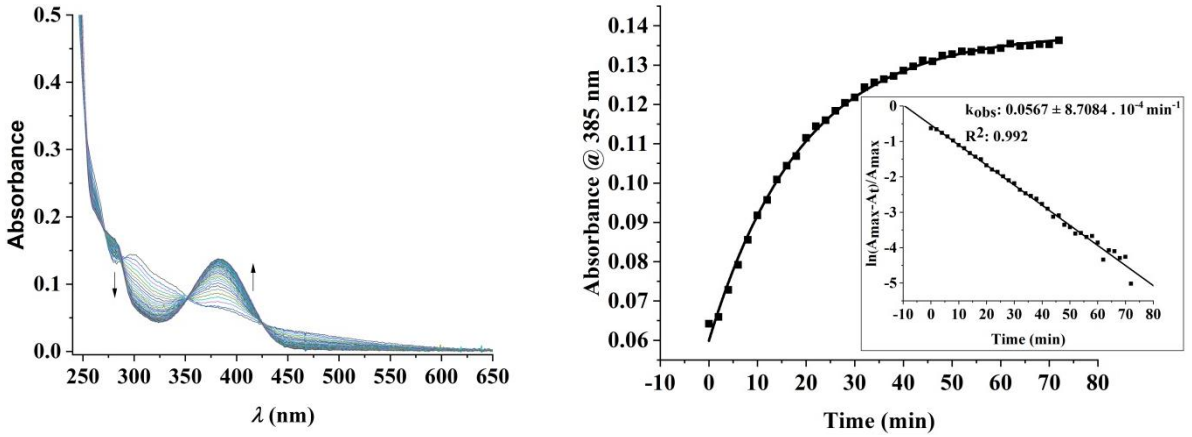

Figure 7. *Left:* Spectral changes of **3** (16 μM) in the presence of PPi (20 equiv) with time at pH 7.4 ([Tris buffer] = 10 mM) *Right:* Change in absorbance of **3** in the presence of PPi (20 equiv) at 385 nm. *Inset:* Plot of $ln(A_{max}-A_t)/A_{max}$ vs time for determining k_{obs}.

10.1002/chem.201905686

Sensing of PPi in foodstuff and biological samples

The applicability of compound **3** for sensing PPi was tested in foodstuff and biological samples. In a proof-of-principle study, we chose to detect PPi alias E450 in baking powder. The latter contains additionally $NaHCO_3$ and starch. Addition of an aqueous sample of baking powder to compound **3** at pH 7.4 ([Tris] = 10 mM) led to an increase of fluorescence at 500 nm suggesting the detection of E450 (Figure 8). This observation was supported by control experiments with HCO_3^- and starch that did not lead to a detectable signal (Figure S20).

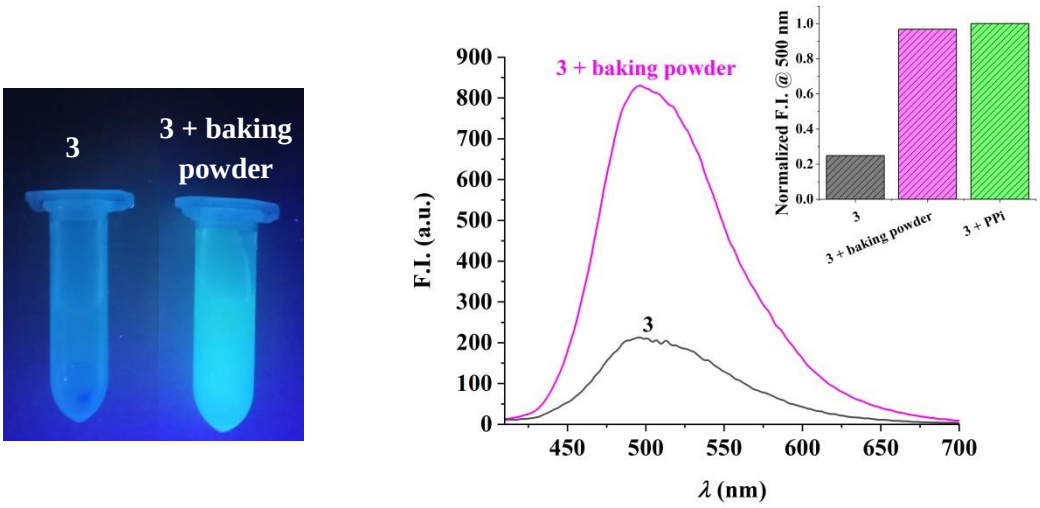

Figure 8. *Left:* Detection of PPi with **3** (16 μM) in an aqueous baking powder solution using a laboratory UV lamp. *Right:* Increase of fluorescence upon addition of an aqueous baking powder solution to **3** (16 μM, λ_{ex} = 385 nm). *Inset:* Comparison of fluorescence intensities of **3** in the absence and presence of baking powder as well as in the presence of PPi (200 μM).

In addition we tested also the applicability of **3** for sensing PPi in HeLa (human cervix adenocarcinoma) cell line. A luminescent cell viability assay (CellTiter Glo®) indicated no cytotoxic effects upon treatment of cells for 1h with a up to 100 μM of **3** (Figure S21). Despite this encouraging result, imaging of PPi with **3** in live HeLa cancer cells with either confocal microscopy or flow cytometry was impeded by the strong autoflourescence of HeLa cells at 500 nm as shown in the supporting information (Figures S22-S24). To overcome this limitation, prove cellular uptake of the probe and its disassembly in the presence of endogenous PPi, we plan to develop and test improved disassembly based probes in the future.

Conclusions:

In this work, we report on three Fe^{III}-salen complexes containing a 3-chloro-5-imine-4-hydroxybenzenesulfonic acid subunit and a modified diamine backbone. We demonstrated that two out of the three metal complexes are demetallated in the presence of (polyoxo)phosphate anions and hydrolyse subsequently into their molecular building blocks. The release of the 3-chloro-5-formyl-4-hydroxybenzenesulfonic acid signaling unit is accompanied by a fluorometric response with an emission at 500 nm. Only one of the two probes was selective for PPi over sixteen other anions. This new probe with an 1,2-propanediamine backbone showed higher selectivity and better sensitivity for PPi compared to a prototype. In particular, the new derivative showed a 155-times better discrimination of PPi over ATP and a 2.3-times higher fluorescence upon disassembly. This probe was also successfully applied for sensing of PPi in foodstuff in a proof-of-principle study with baking powder. Studies with HeLa cells demonstrated that the probe was not suitable for cellular applications due to an overlap of the emission spectra of the compound with the high autofluorescence of HeLa cells. This observation has to be considered in future probe design.

Conflict of Interest:

There are no conflicts to declare.

Acknowledgements:

We acknowledge financial and general support by the Department of Chemistry of the University of Zurich. HR-ESI-MS spectra were kindly recorded by Urs Stalder and Prof. Dr. Laurent Bigler. This work was financially supported by a grant of the Swiss National Science Foundation (F.Z.: grant-no.: 200021_169216), by an ERC Consolidator Grant PhotoMedMet to G.G. (GA 681679) and has received support under the program “Investissements d’Avenir” launched by the French Government and implemented by the ANR with the reference ANR-10-IDEX-0001-02 PSL (G.G.).

1. A. E. Hargrove, S. Nieto, T. Zhang, J. L. Sessler and E. V. Anslyn, *Chem. Rev.*, 2011, **111**, 6603-6782.
2. F. Zelder, *Chem. Commun.*, 2015, **51**, 14004-14017.
3. L. Stryer, *Biochemistry*, W. H. Freeman and Company, New York, third edn., 1988.

4. W. N. Lipscomb and N. Sträter, *Chem. Rev.*, 1996, **96**, 2375-2434.
5. J. K. Heinonen, *Biological Role of Inorganic Pyrophosphate*, Kluwer Academic Publishers, Boston, 2001.
6. R. Kramer, *Biochem. Biophys. Res. Commun.*, 1985, **127**, 129-135.
7. Food Standards Agency, Food Additives Legislation Guidance to Compliance, (https://www.food.gov.uk/sites/default/files/media/document/food-additives-legislation-guidance-to-compliance.pdf).
8. E. Ritz, K. Hahn, M. Ketteler, M. K. Kuhlmann and J. Mann, *Dtsch. Arztebl. Int.*, 2012, **109**, 49-55.
9. Institute of Medicine, *Dietary Reference Intakes for Calcium, Phosphorus, Magnesium, Vitamin D and Fluoride*, The National Academies Press, Washington, DC, 1997.
10. R. Dhingra, L. M. Sullivan, C. S. Fox, T. J. Wang, R. B. D'Agostino, Sr, J. M. Gaziano and R. S. Vasan, *Arch. Intern. Med.*, 2007, **167**, 879-885.
11. U. Trautvetter, B. Ditscheid, G. Jahreis and M. Glei, *Nutrients*, 2018, **10**, 171.
12. S. Bhowmik, B. N. Ghosh, V. Marjomäki and K. Rissanen, *J. Am. Chem. Soc.*, 2014, **136**, 5543-5546.
13. N. Kumari and F. Zelder, *Chem. Commun.*, 2015, **51**, 17170-17173.
14. R. R. Mittapalli, S. S. R. Namashivaya, A. S. Oshchepkov, E. Kuczyńska and E. A. Kataev, *Chem. Commun.*, 2017, **53**, 4822-4825.
15. S. K. Kim, D. H. Lee, J.-I. Hong and J. Yoon, *Acc. Chem. Res.*, 2009, **42**, 23-31.
16. H. J. Jessen, *Phosphate Labeling and Sensing in Chemical Biology*, Springer International Publishing, Switzerland, 2017.
17. S. Pal, T. K. Ghosh, R. Ghosh, S. Mondal and P. Ghosh, *Coord. Chem. Rev.*, 2020, **405**, 213128.
18. S. Lee, K. K. Y. Yuen, K. A. Jolliffe and J. Yoon, *Chem. Soc. Rev.*, 2015, **44**, 1749-1762.
19. D. H. Vance and A. W. Czarnik, *J. Am. Chem. Soc.*, 1994, **116**, 9397-9398.
20. D. H. Lee, S. Y. Kim and J.-I. Hong, *Angew. Chem. Int. Ed.*, 2004, **43**, 4777-4780.
21. H. K. Cho, D. H. Lee and J.-I. Hong, *Chem. Commun.*, 2005, **13**, 1690-1692.
22. M. J. McDonough, A. J. Reynolds, W. Y. G. Lee and K. A. Jolliffe, *Chem. Commun.*, 2006, **28**, 2971-2973.
23. S. Dey and P. K. Sukul, *ACS Omega*, 2019, **4**, 16191-16200.
24. V. Kumar, P. Kumar, S. Kumar, D. Singhal and R. Gupta, *Inorg. Chem.*, 2019, **58**, 10364-10376.
25. M. Strianese, S. Milione, A. Maranzana, A. Grassi and C. Pellecchia, *Chem. Commun.*, 2012, **48**, 11419-11421.
26. M. Cano, L. Rodríguez, J. C. Lima, F. Pina, A. Dalla Cort, C. Pasquini and L. Schiaffino, *Inorg. Chem.*, 2009, **48**, 6229-6235.
27. N. Kumari, H. Huang, H. Chao, G. Gasser and F. Zelder, *ChemBioChem.*, 2016, **17**, 1211-1215.
28. A. Erxleben, *Inorg. Chim. Acta*, 2018, **472**, 40-57.
29. D. Xie, J. Jing, Y.-B. Cai, J. Tang, J.-J. Chen and J.-L. Zhang, *Chem. Sci.*, 2014, **5**, 2318-2327.
30. I. P. Oliveri, G. Forte, G. Consiglio, S. Failla and S. Di Bella, *Inorg. Chem.*, 2017, **56**, 14206-14213.
31. J. Chan, S. C. Dodani and C. J. Chang, *Nature Chem.*, 2012, **4**, 973-984.
32. Z. Xu and L. Xu, *Chem. Commun.*, 2016, **52**, 1094-1119.
33. M. Sayar, E. Karakuş, T. Güner, B. Yildiz, U. H. Yildiz and M. Emrullahoğlu, *Chem. Eur. J.*, 2018, **24**, 3136-3140.
34. B. W. Michel, A. R. Lippert and C. J. Chang, *J. Am. Chem. Soc.*, 2012, **134**, 15668-15671.
35. J. Liu, J. Cheng, X. Ma, X. Zhou and H. J. R. o. C. I. Xiang, *Res. Chem. Intermed*, 2016, **42**, 5027-5048.
36. A. Salanti, M. Orlandi, E.-L. Tolppa and L. Zoia, *Int. J. Mol. Sci.*, 2010, **11**, 912-926.
37. E. B. Hager, B. C. E. Makhubela and G. S. Smith, *Dalton Trans.*, 2012, **41**, 13927-13935.
38. V. K. Sivasubramanian, M. Ganesan, S. Rajagopal and R. Ramaraj, *J. Org. Chem.*, 2002, **67**, 1506-1514.
39. H. Fujii and Y. Funahashi, *Angew. Chem. Int. Ed.*, 2002, **41**, 3638-3641.

40. H. Fujii and Y. Funahashi, *Angew. Chem.*, 2002, **114**, 3790-3793.
41. J. W. Pyrz, A. L. Roe, L. J. Stern and L. Que, *J. Am. Chem. Soc.*, 1985, **107**, 614-620.
42. T. S. Lange, K. K. Kim, R. K. Singh, R. M. Strongin, C. K. McCourt and L. Brard, *PLoS One*, 2008, **3**, e2303.
43. N. Graf and S. J. Lippard, *Adv. Drug Delivery Rev.*, 2012, **64**, 993-1004.
44. I. Würtenberger, V. Follia, F. Lerch, C. Cwikla, N. Fahrner, C. Kalchschmidt, B. Flögel, B. Kircher and R. Gust, *J. Med. Chem.*, 2015, **58**, 588-597.
45. L. Mao, K. Yamamoto, W. Zhou and L. Jin, *Electroanalysis*, 2000, **12**, 72-77.
46. P. G. Cozzi, *Chem. Soc. Rev.*, 2004, **33**, 410-421.
47. S. Shaw and J. D. White, *J. Am. Chem. Soc.*, 2014, **136**, 13578-13581.
48. B. Spingler, S. Schnidrig, T. Todorova and F. Wild, *CrystEngComm.*, 2012, **14**, 751-757.

10.1002/chem.201905686

Table of Contents

We describe a Fe^{III}-salen based probe for the selective fluorometric detection of pyrophosphate alias E450 in baking powder via a disassembly approach.